Synthetic-aperture experiment in the visible with on-axis digital heterodyne holography

Frédérique Le Clerc, Michel Gross, Laurent Collot

Synthetic-aperture experiment in the visible with on-axis digital heterodyne holography

F. Le clerc and M. Gross

Laboratoire Kastler-Brossel,
UMR 8552 CNRS, Ecole Normale Supérieure,
Université Pierre et Marie Curie,
24 rue Lhomond 75231 Paris cedex 05 France

L. Collot

Thomson CSF Optronique, Rue Guynemer B.P. 55,
78 283 Guyancourt, France

We have developed a new on-axis digital holographic technique, heterodyne holography. The resolution of this technique is limited mainly by the amount of data recorded on two-dimensional photodetectors, i.e., the number of pixels and their size. We demonstrate that it is possible to increase the resolution linearly with the amount of recorded data by aperture synthesis as done in the radar technique but with an optical holographic field.

A synthetic aperture is used in a technique for signal processing that combines signals acquired by a moving detector into a unique signal field map that permits higher-resolution image reconstruction. This technique, which has been known for 30 years in the visible [1] and the near IR [2], is used extensively for synthetic-aperture radar [3] and synthetic-aperture sonar [4]. More recently, synthetic-aperture telescopes, in which several small telescopes collect optical fields that are combined to yield higher-resolution images, have been developed [5]. For all these syntheticaperture techniques the ultimate angular resolution λ/D' corresponds to the equivalent aperture size D', i.e., to the detector displacement or to the telescopes maximum relative distance.

Digital holography permits the complex optical field to be measured directly and images to be obtained by calculation of the field in the plane of the object, but, for both off-axis [6] and on-axis [7, 8] holography, the finite number of recorded pixels limits the resolution (which is nevertheless better in the on-axis case). To overcome this limitation it is natural to construct a holographic synthetic aperture by recording several different holograms of the same object and reconstructing the image from all of them. Here we use our heterodyne holography setup [9] to illustrate this idea. Using holograms that correspond to various positions of the spatial filter, which selects the photons that fulfill the sampling condition, we performed an aperture synthesis in Fourier space. For a short-distance object, we demonstrate the synthetic-aperture effect by overcoming the limit on pixel-size resolution, which is that of one hologram [9].

Figure 1 is a schematic of our experiment. The signal field, at wavelength l, which is scattered by a coherently illuminated object, passes through a spatial filter system, that comprises objectives O1 ($f_1 = 50$ mm) and O2 ($f_2 = 25$ mm), with rectangular aperture spatial filter (SF) in their common focal plane. O1 transforms field
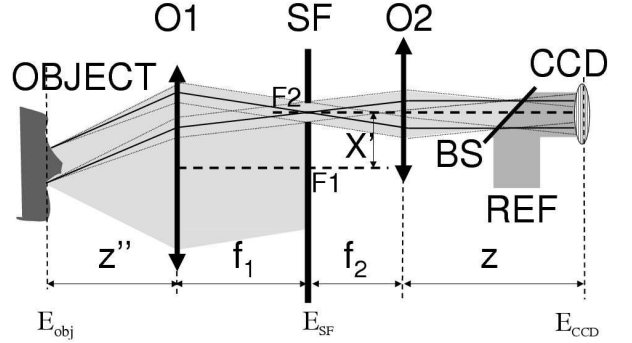

FIG. 1: Spatial filter system composed of lenses O1 and O2, rectangular spatial filter SF, beam splitter BS and a CCD camera.

E_{obj} in the plane of the object into its k-space components E_{SF} in the SF plane, whereas O2 backtransforms E_{SF} into E_{CCD} on the CCD. O2, SF, and the CCD, which can be moved, are kept aligned, and the field, when it reaches the CCD, propagates nearly parallel to the reference beam (REF). In Fig. 1 and in what follows, the $x''y''$ (object plane) coordinates refer to the O1 fixed axis; xy (CCD plane) and $x'y'$ (SF plane) coordinates refer to the SF, CCD, and O2 moving axis, which is shifted by X', Y' with respect to O1. Double, single, and no primes are used for the object, SF, and CCD planes, respectively. The resolution on the reconstructed object is $r'' = \lambda f_1/D'$, where D' is the size of the SF plane region where E_{SF} is measured. To avoid aliasing in the reconstructed images, D' must fulfill the sampling condition $D' < D_{SF} = \lambda f_2/d$, which corresponds to pixel size d. In the best case, $D' = D_{SF}$, resolution $r'' = df_1/f_2$ is equal to the size of the CCD pixels enlarged by the O1O2 expansion factor. We recorded holograms for sev-

eral positions of the SF, CCD, and O2 moving axis and determined E_{SF} over a displacement of the SF Fourier plane of size $D' = G.D_{SF}$ ($G \gg 1$).

For a given moving axis position (X'_i, Y'_j), the field $(E_{SF})_{i,j}$ that is selected by SF is related to the measured CCD field $(E_{CCD})_{i,j}$ by

$$(E_{SF})_{i,j} = (\delta_{X'_i,Y'_j}) \otimes \left[\prod_{D_{SF}} O_{f_2,z}(E_{CCD})_{i,j} \right] \quad (1)$$

where z is the CCDO2 distance (Fig. 1) and $O_{f,z}$ is the lens operator that transforms field E_{CCD} at lens distance z into focal-plane field E_{SF}. The $\prod_{D_{SF}}$ two-dimensional gate operator accounts for the SF aperture and defines the size of the k-space selected zone. These operators work within the moving coordinates of O2. Two-dimensional Dirac function δ and convolution operator $\otimes$ perform the X'_i, Y'_j displacement to yield E_{SF} within the fixed coordinates of O1. Operator $O_{f,z}$ can be expressed [10] as

$$O_{f,z} = \int_{-\infty}^{-\infty} dx \int_{-\infty}^{-\infty} dy$$
$$\times \exp[i2\pi(xx' + yy')/\lambda f]\, E(x,y) \quad (2)$$

where $O_{f,D}$ Fourier transforms $E(x,y)$, which is multiplied by a quadratic phase function that corresponds to $z - f$ propagation. To determine E_{SF} over a wider region it is necessary to combine the SF fields $(E_{SF})_{i,j}$ that correspond to various SF positions i,j:

$$E_{SF} = \sum_i^G \sum_j^G (E_{SF})_{i,j} \quad (3)$$
$$= \sum_i^G \sum_j^G (\delta_{X'_i,Y'_j}) \otimes \left[\prod_{D_{SF}} O_{f_2,z}(E_{CCD})_{i,j} \right]$$

If the selected SF zones are contiguous and do not overlap, $X'_{i+1} - X'_i = D_{SF}$ et $Y'_{j+1} - Y'_j = D_{SF}$, the wider region is G times wider than for a single hologram.

In our experiment, field $(E_{CCD})_{i,j}$ is measured in discrete pixels, and the CCD measured pixels are inserted into an $N \times N$ empty grid of step d. For fast Fourier transforms (FFTs), N is a factor of 2 larger than the CCD pixel number. In the SF plane, field $(E_{SF})_{i,j}$ is a FFT calculated on a grid of step d'. Inasmuch as FFT steps d and d' obey $Ndd' = \lambda f_2$, the SF grids full size is $Nd' = D_{SF}$. The $\prod_{D_{SF}}$ gate function is thus accounted for by the FFT. To obtain the sum over field $(E_{SF})_{i,j}$ that yields E_{SF} [Eq. 3], we insert each $N \times N$ small matrix $(E_{SF})_{i,j}$ within an E_{SF} $N' \times N'$ large matrix ($N' = GN$). Accounting for the X'_i, Y'_j translation, the indices within the large matrix of the center of the small matrix i^{th}, j^{th} are X'_i/d' and y'_j/d'. Because the object is at a distance z'' of O1 (focal f_1), we calculate E_{obj} by applying to E_{SF} the reverse lens operator $O^{-1}_{f_1,z''}$ whose expression can be deduced from Eq. 2. Because O^{-1}
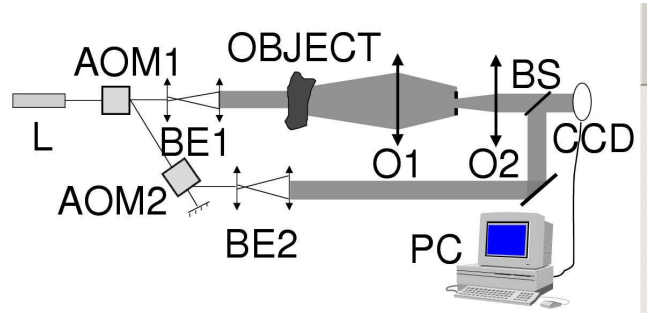

FIG. 2: Heterodyne holography setup with laser L, accousto-optic modulators AOM1 and AOM2, beam expanders BE1 and BE2, objectives O1 and O2, beam splitter BS, a CCD camera, and computer PC.

involves a FFT, object plane grid step d'', which obeys $N'd'd'' = \lambda f_1$, decreases linearly with G: $d'' = \lambda f/f_2 G$. In measuring CCD field E_{CCD} that corresponds to different, nonoverlapping positions of SF, one can thus calculate object plane field E_{obj} with a resolution and a pixel size that improve linearly with the amount of data acquired.

Figure 2 shows our experimental setup in details. Laser L (633-nm HeNe laser, or 850-nm laser diode) is split into two beams (object and reference), which are combined by a beam splitter (BS) in the CCD camera. Two acousto-optic modulators (AOM1 and AOM2) are used for shifting the reference beam by $\delta f = 6.25$ Hz (25% of the CCD image frequency). A frame grabber and a Pentium II computer record the CCD-modulated interference patterns and calculate complex field E_{CCD} in the CCD. A step motors (0.1-μm step) allows O2, the BS, the SF aperture ($D_{SF} = 1.84$, 1.9 mm in the x and y directions) and the CCD, keeping them in alignment.

The first object studied is a U.S. Air Force test target lightened by a static speckle pattern emerging from a ground-glass plate illuminated by the HeNe laser. In the CCD plane, the calculation step $d_x = 8.42\mu$m and $d_y = 8.3\mu$m is equal to the pixel size. The matrix dimension ($N \times N$, with $N = 1024$) is larger than the CCD dimension 768×576. In the SF plane, the grid step is $d'_x = 1.84\mu$m and $d'_y = 1.86\mu$m. The CCDO2 distance is $z = f_2 + 6.87$ cm, and the object O1 distance is $z'' \approx 5$ cm. To improve the resolution by a factor $G = 4$ in the x'' direction we use a synthetic-aperture grid dimension of $N' \times N$, with $N' = 4N = 4096$. In the object plane, the grid step is then four times smaller in the x'' direction ($d''_x = d_x/4 = 4.21\mu$m) and is unchanged in the y'' direction ($d''_y = 16.6\mu$m).

We calculated for a single hologram the U.S. Air Forcer intensity image ($N \times N = 1024 \times 1024$ pixels, or 17.2 mm $\times$ 17 mm). The central part of the image is shown in Fig. 3(a). The image resolution and the speckle size, which depend on k-space extension $D' = D_{SF}$, should both equal $d'' = (f_1/f_2)d$. In our case, a low-pass filter, in-

FIG. 4: Cut in intensity for a 30-mm hole in the x and y directions. Points, experimental synthetic-aperture reconstruction; and curves, expected theoretical shapes. Dark filled squares and the solid curve correspond to the x'' cut; lighter filled circles and the dashed curve correspond to the y'' cut (synthetic aperture is formed in the x'' direction).
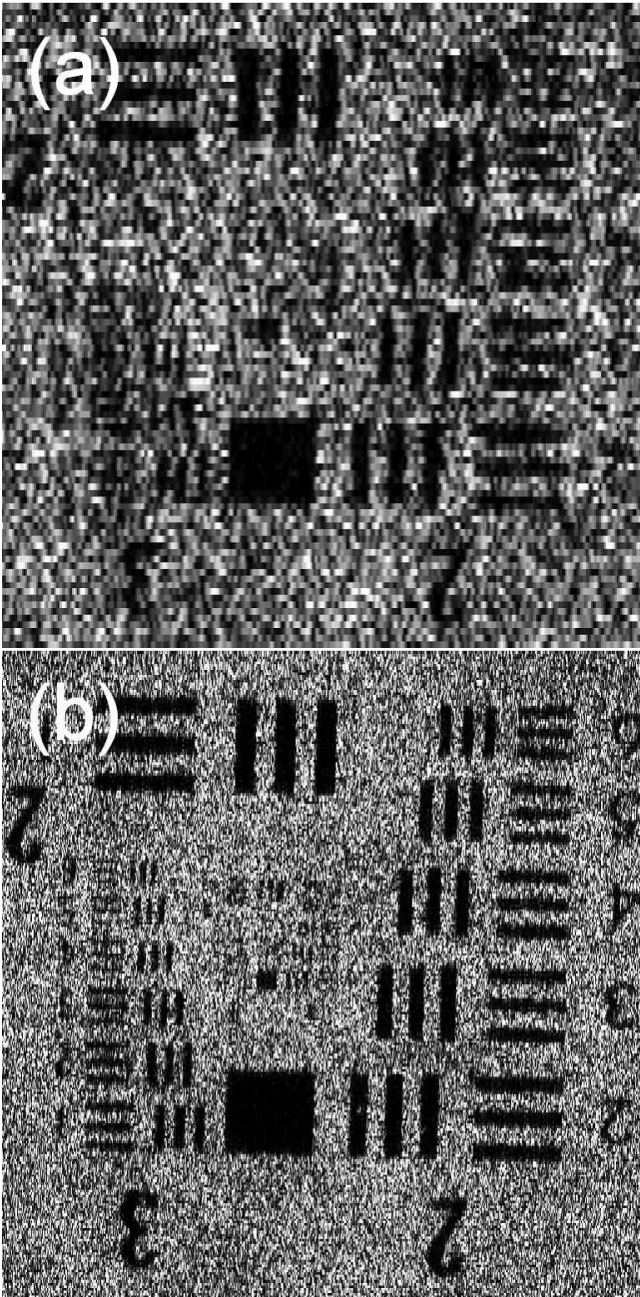

FIG. 3: (a), (b), the center of the image of a U.S. Air Force test target obtained without and with a synthetic aperture, respectively. The reconstruction was performed with 1024×1024 and 4096×1024 pixels, respectively; it corresponds to a 17.2 mm $\times$ 17 mm image. The viewed zone is 4.03 mm $\times$ 3.98 mm.

ternal to the camera, lowers the bandwidth of the analog video stream of data, which degrades the resolution and enlarges the speckle size by a factor of ~ 2 in the x'' direction.

When the synthetic-aperture algorithm is applied, because the BS moves with SF the reference optical path length changes for each SF position. Each measured
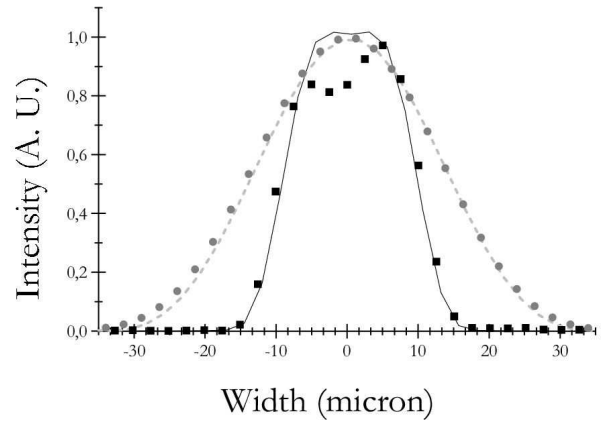
E_{CCD} field map is thus shifted by an unknown phase. To determine the phase correction we acquire holograms such that the zones covered by the aperture overlap for two consecutive SF positions $(X'_{i+1} - X'_i) < DSF$ ($i = 1...21$ and $X'_{i+1} - X'_i = 250\mu$m in our experiment). We assume thus that fields $(E_{SF})_{i+1,j}$ are equal in the overlapping region, and we determine the phase by maximizing, in the overlapping region, the $(E_{SF})_{i,j}$ to $(E_{SF})_{i+1,j}$ field correlation, which we found to be 90% at maximum. We calibrated the $X'_{i+1} - X'_i$ transition (135 pixels) and the CCDO2 distance [$z = 6.87$ mm in the quadratic phase factor of Eq. 2] by this optimization process.

We calculated the synthetic-aperture reconstructed image (4096×1024 pixels, 17.2 mm $\times$ 17 mm) when the SF, O2, the BS, and the CCD are X' translated over $D' = 5$ mm in 21 250-μm steps. The image center is shown in Fig. 3(b). The motor calibration yields a relative translation of 134.8 pixels, in good agreement with the value obtained by correlation. As expected, the synthetic-aperture image exhibits better resolution and smaller speckle size. If the BS phase-shift correction is not made, the speckle size, which depends on the field extension in k-space $\sim GD_{SF}$, is the same, but the resolution, which depends on the k-space field coherence length ($\sim GD_{SF}$ with correction and $\sim D_{SF}$ without), is lower. The image contrast is thus lower.

To perform a quantitative analysis of our synthetic-aperture technique, we studied a narrow hole of diameter $\emptyset = 30$ mm located at $z = 5.5$ cm in front of the SF. The hole is backilluminated by an 850-nm laser diode. The SF, O2, the BS, and the CCD are X' translated over $D' = 5$ mm in 250-μm steps that correspond to 101.6 pixels. O1 is removed, and two Fourier transforms [9] propagate the field from the SF plane to the object plane

such that the grid size ($d'_x = d''_x = 2.46\mu$m, $d'_y = d''_y = 2.5\mu$m is the same in both planes. Figure 4 presents, in the x'' and y'' directions, the reconstructed intensities (points) compared with the theoretical intensities (solid curve) that account for pixel averaging and diffraction. As expected, the edges are sharper in the x'' direction. For both x'' and y'', the agreement with the experimental points is excellent. This experiment, performed without O1, can be interpreted as yielding the synthetic aperture in real space for field E_{SF} that we obtained by Fourier transforming ECCD. The synthetic aperture here allows the images angular resolution to be increased to reach grid step limit d0 for the resolution on the image. One could also use the real-space synthetic aperture in the CCD plane11 without transforming E_{CCD} into E_{SF}, but the ultimate resolution limit d is much less $d' \ll d$.

The experiments presented here are examples of ways in which synthetic apertures are obtained in both real and Fourier space. In Fourier space, the synthesis allows either the field of view in the far field [9] (with respect to Nd^2/λ) or the resolution for the near field (U.S. Air Force experiment) to be improved. In real space, the synthesis improves either the field of view (near field) or the resolution (far field). In the experiment with holes, the pixel size of field E_{SF}, d', is small, and the hole is pushed into the far field $z'' \gg Nd'^2\lambda$. Note that for both the U.S. Air Force experiment of Binet et al. [11] and the hole experiment, the synthesis yields better resolution, not the enlargement of the field of view that could be obtained by a simple scanning method.

[1] G. O. Reynolds and D. J. Cronin. Imaging with optical synthetic apertures (mills-cross analog). *JOSA*, 60(5):634–640, 1970.

[2] E.L. Dereniak. Application of a synthetic aperture optical system to infrared imaging. *Applied Optics*, 12(3):487–492, 1973.

[3] LJ Cutrona. *Radar handbook*, chapter Synthetic aperture radar, pages 2333–2346. New York: McGraw-Hill, 1990.

[4] Special issue on accoustic synthetic aperture processing. *IEEE J. Ocean. Eng.*, 17:1, 1992.

[5] JE Baldwin, MG Beckett, RC Boysen, D. Burns, DF Buscher, GC Cox, CA Haniff, CD Mackay, NS Nightingale, J. Rogers, et al. The first images from an optical aperture synthesis array: mapping of capella with coast at two epochs. *Astronomy and Astrophysics*, 306:L13, 1996.

[6] U. Schnars. Direct phase determination in hologram interferometry with use of digitally recorded holograms. *JOSA A*, 11(7):2011–2015, 1994.

[7] A.J. Decker, Y.H. Pao, and PC Claspy. Electronic heterodyne recording and processing of optical holograms using phase modulated reference waves. *Applied Optics*, 17(6):917–921, 1978.

[8] T. Zhang and I. Yamaguchi. Three-dimensional microscopy with phase-shifting digital holography. *Optics letters*, 23(15):1221–1223, 1998.

[9] F. Le Clerc, L. Collot, and M. Gross. Numerical heterodyne holography with two-dimensional photodetector arrays. *Optics Letters*, 25(10):716–718, 2000.

[10] J.W. Goodman. *Introduction to Fourier optics. Chap. 3.* McGraw-Hill, San Francisco, Calif, 1968.

[11] R. Binet, J. Colineau, and J.C. Lehureau. Short-range synthetic aperture imaging at 633 nm by digital holography. *Applied optics*, 41(23):4775–4782, 2002.